

This article was downloaded by:

On: 26 January 2011

Access details: *Access Details: Free Access*

Publisher *Taylor & Francis*

Informa Ltd Registered in England and Wales Registered Number: 1072954 Registered office: Mortimer House, 37-41 Mortimer Street, London W1T 3JH, UK



Liquid Crystals

Publication details, including instructions for authors and subscription information:

<http://www.informaworld.com/smpp/title~content=t713926090>

Smectic A twist grain boundary phase in three new series with chiral (L) lactic acid derivatives

L. Navailles^a; H. T. Nguyen^a; P. Barois^a; C. Destrade^a; N. Isaert^b

^a Centre de Recherche Paul Pascal, Pessac Cedex, France ^b Laboratoire de Dynamique et Structure des Matériaux Moléculaires, (U.R.A., CNRS No. 801), Université de Lille 1, Villeneuve d'Ascq Cedex, France

To cite this Article Navailles, L. , Nguyen, H. T. , Barois, P. , Destrade, C. and Isaert, N.(1993) 'Smectic A twist grain boundary phase in three new series with chiral (L) lactic acid derivatives', *Liquid Crystals*, 15: 4, 479 – 495

To link to this Article: DOI: 10.1080/02678299308036468

URL: <http://dx.doi.org/10.1080/02678299308036468>

PLEASE SCROLL DOWN FOR ARTICLE

Full terms and conditions of use: <http://www.informaworld.com/terms-and-conditions-of-access.pdf>

This article may be used for research, teaching and private study purposes. Any substantial or systematic reproduction, re-distribution, re-selling, loan or sub-licensing, systematic supply or distribution in any form to anyone is expressly forbidden.

The publisher does not give any warranty express or implied or make any representation that the contents will be complete or accurate or up to date. The accuracy of any instructions, formulae and drug doses should be independently verified with primary sources. The publisher shall not be liable for any loss, actions, claims, proceedings, demand or costs or damages whatsoever or howsoever caused arising directly or indirectly in connection with or arising out of the use of this material.

Smectic A twist grain boundary phase in three new series with chiral (L) lactic acid derivatives

by L. NAVAILLES, H. T. NGUYEN*, P. BAROIS and C. DESTRADE

Centre de Recherche Paul Pascal, Avenue A. Schweitzer,
F 33600 Pessac Cedex, France

and N. ISAERT

Laboratoire de Dynamique et Structure des Matériaux Moléculaires,
(U.R.A., CNRS No. 801), Université de Lille 1, U.F.R. de Physique,
F59655 Villeneuve d'Ascq Cedex, France

(Received 23 February 1993; accepted 9 May 1993)

Three new series with a tolane core and a chiral L-lactic acid moiety have been synthesized. The theoretically predicted S_A - TGB_A - N^* phase sequence is found in several compounds with short chains. The smectic A twist grain boundary phase (TGB_A) obtained with a cholesteric texture, is characterized by different techniques. Helical pitch measurements were performed using Grandjean-Cano wedges or homeotropic drops. All pitch values are lower than those found in previously reported series exhibiting the TGB_A phase. Ferroelectric smectic C (S_C^*) phases appear with long chains and have striated fan-shaped or pseudo-homeotropic textures. Electro-optical properties of the S_C^* phase were studied with the classical SSFLC geometry. We observed high polarization, slow response time and a saturated tilt angle of 20° . These results are comparable with previous studies.

1. Introduction

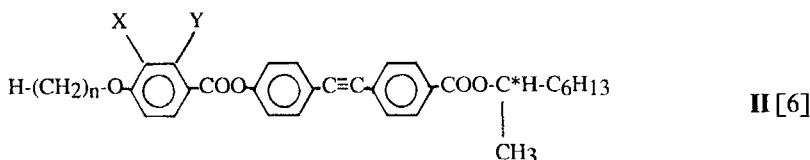
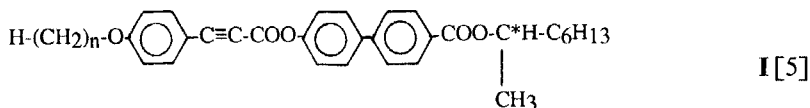
In 1972, de Gennes [1] established a strong analogy between the nematic (N) to smectic A (S_A) transition in liquid crystals and the normal to superconductor transition in metals. In the case of a mesogenic material constituted of chiral molecules, he predicted the existence of a twisted smectic phase, between the cholesteric (N^*) and the smectic A phase, analogous to the Abrikosov phase in type II superconductors.

In 1988, Renn and Lubensky [2] proposed a theoretical structure of this new phase called the twist grain boundary (TGB) smectic A phase. This highly dislocated S_A phase consists of a twisted array of infinite two dimensional smectic slabs which are stacked along the pitch axis. Adjacent slabs are separated by grain boundaries which consist of a grid of parallel equispaced screw dislocation lines. These grids, like the smectic slabs, form a twisted stack.

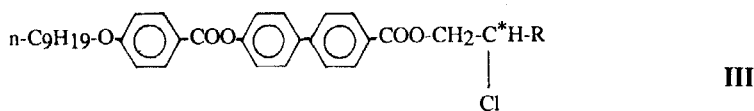
According to Renn and Lubensky [3] and Renn [4], three different TGB smectics have to be distinguished: TGB_A , TGB_C and TGB_C^* . They are constituted of S_A , S_C and helical S_C^* slabs respectively.

*Author for correspondence.

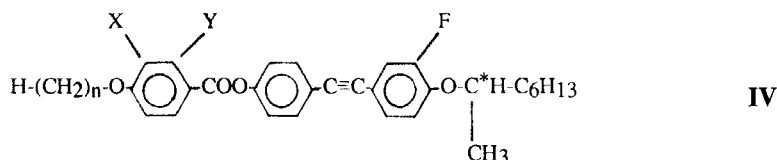
So far, the TGB_A phase has been found in different series



These series have similar molecular structures, but the position of the linking group $-\text{C}\equiv\text{C}-$ is different. They exhibit the same mesomorphic properties with the sequence: crystalline phase (C)– S_C^* – TGB_A –isotropic phase (I) for long chain homologues. Let us point out that this sequence with the TGB_A phase is not the sequence predicted by de Gennes [1] or Renn and Lubensky [2], i.e. S_A – TGB_A – N^* . This last sequence was first found by Lavrentovich *et al.* [7], in a mixture of cholesteryl *n*-nonanoate and *n*-nonyloxybenzoic acid in a 7:3 weight proportion, then by Slaney *et al.* [8] in a pure compound in which the chiral secondary alcohol was replaced by a chiral primary alcohol derived from L-amino acids.



In these three series, the chiral alcohol chains are linked to the core by the $-\text{COO}-$ group which favours the formation of the S_A phase. In 1992, Bouchta *et al.* [9], replaced the linking group $-\text{COO}-$ by $-\text{O}-$ and put in an electron attracting group (F) *ortho*- to the chiral alkyloxy chain in order to obtain the TGB phases. Their series has the general formula

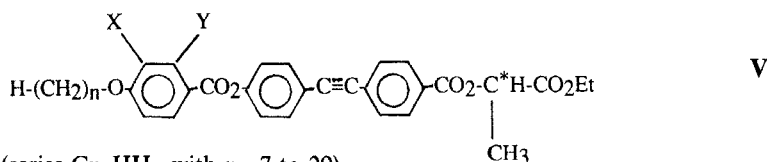


The series ($X = \text{H}$, $Y = \text{H}$) and ($X = \text{F}$, $Y = \text{H}$) display the phase sequence



whereas the tilted TGB_C phase was found in the ($X = \text{F}$, $Y = \text{F}$) series [10].

In this study, we examine the properties of three new series obtained by replacing the chiral alcohol by another derived from L-lactic acid. The tolane core and the $-\text{COO}-$ linking group are preserved. The new series has the general formula:

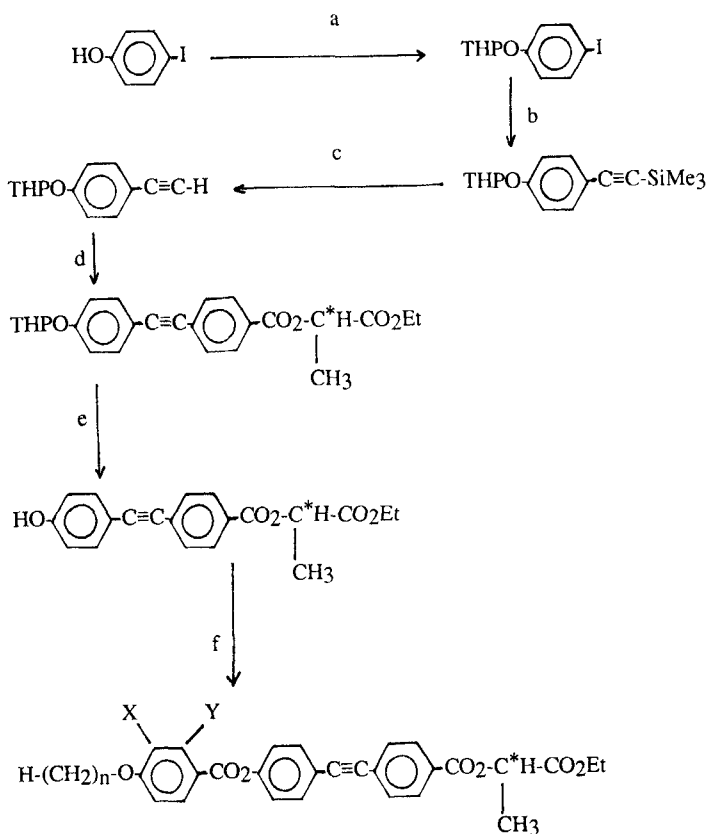


$X = Y = \text{H}$ (series $C_n\text{-HH-}$ with $n = 7$ to 20)
 $X = \text{F}$, $Y = \text{H}$ (series $C_n\text{-FH-}$ with $n = 7$ to 20)
 $X = Y = \text{F}$ (series $C_n\text{-FF-}$ with $n = 7$ to 20)

This paper is organized as follows: the chemical synthesis is briefly presented in § 2. Mesomorphic properties such as those observed by optical microscopy, and racemic mixture and calorimetric studies are reported in § 3. Section 4 is devoted to X-ray diffraction studies and § 5 to helical pitch measurements. Finally, electro-optical properties of the S_C^{*} phase are given in § 6.

2. Synthesis

The compounds of series C_n-HH-, C_n-FH- and C_n-FF- were prepared following the scheme:



(a) DHP, PTSA, CH₂Cl₂.

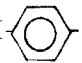
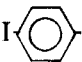
(b) HC≡CSiMe₃, PdCl₂, Cu(AcO)₂, H₂O, Ph₃P, iPr₂NH.

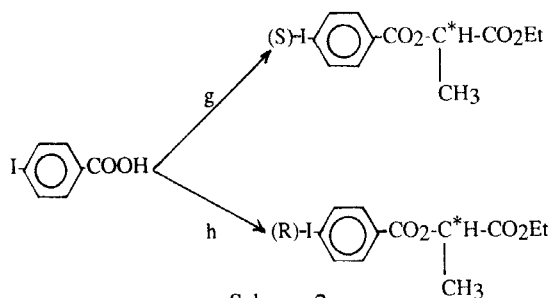
(c) NaOH 50 per cent, MeOH, THF.

(d) $\text{I-C}_6\text{H}_4\text{-CO}_2\text{-C}^*\text{H-CO}_2\text{Et}$, PdCl₂, Cu(AcO)₂, H₂O, Ph₃P, iPr₂NH.
|
CH₃

(e) PTSA, THF, MeOH.

(f) $\text{H-(CH}_2)_n\text{-O-C}_6\text{H}_3(\text{X,Y)-COOH}$, DCC, DMAP, CH₂Cl₂

The (R)- and (S)-I--COO-C*H-CO₂Et were prepared from I--CO₂H and (S)-CH₃-C*H-CO₂Et following two different reactions (scheme 2):



(g) (S)-CH₃-C*H-CO₂Et, DCC, DMAP, CH₂Cl₂.

(h) (S)-CH₃-C*H-CO₂Et, Ph₃P, DEAD, CH₂Cl₂.

Details of the synthesis are reported in the experimental section.

3. Mesomorphic properties

All the new compounds of series *C_n-HH-*, *C_n-FH-*, and *C_n-FF-* are mesomorphic. The liquid crystal transition temperatures and enthalpies were determined both by thermal optical microscopy (Mettler FP 52) and differential scanning calorimetry (Perkin-Elmer [7]).

The phase sequences and the corresponding transition temperatures for these new series are reported in tables 1 (a), (b) and (c) and figures 1 (a), (b) and (c).

Table 1. (a) Transition temperatures (°C) of compounds of series *C_n-HH-*. The meanings of the signs used in this table are: C, crystalline phase; I, isotropic phase; S_A, smectic A phase; S_C^{*}, helical smectic C phase; TGB_A, twist grain boundary smectic A phase; N*, cholesteric phase; BPI, blue phase I; BPIII, blue phase III; ●, the phase exists; —, the phase does not exist.

<i>n</i>	C	S _C [*]	S _A	TGB _A	N*	BPI	BPIII	I							
7	●	93.8	—	●	132.7	—	●	153.8	●	157	—	●			
8	●	113	—	●	139	—	●	152.2	●	153.2	●	155.2	●		
9	●	99	—	●	133.9	—	●	144.5	●	146	●	148.4	●		
10	●	86.7	—	●	136.4	—	●	144	●	145.6	●	147.8	●		
11	●	89.3	—	●	133.5	—	●	138.5	●	140.3	●	142.6	●		
12	●	90	—	●	131	●	131.6	●	134.9	●	136.9	●	139.7	●	
14	●	80	●	101	●	127.1	●	128.2	●	129.1	●	130.4	●	133.1	●
16	●	87.6	●	106	●	123.1	●	124	●	125.2	●	126.2	●	128.6	●
18	●	92	●	103	●	119.7	●	120.8	●	121.7	—	●	123.5	●	
20	●	97.6	●	104	—	●	117	●	118.8	—	●	119.8	●		

Table 1. (b) Transition temperatures (°C) of compounds of series C_n-FH-. The meanings of the signs used in this table are: C, crystalline phase; I, isotropic phase; S_A, smectic A phase; S_C^{*}, helical smectic C phase; TGB_A, twist boundary smectic A phase; N*, cholesteric phase; BPI, blue phase I; BPIII, blue phase III; ●, the phase exists; —, the phase does not exist.

<i>n</i>	C	S _C [*]	S _A	TGB _A	N*	BPI	BPIII	I
7	● 78.4	—	● 116.5	—	● 131.1	● 132.8	● 136	●
8	● 95.5	—	● 119.7	—	● 130.7	● 132.4	● 135.1	●
9	● 93.5	—	● 115.9	● 116.4	● 124.8	● 126.9	● 129.5	●
0	● 83.8	—	● 117.5	● 118.4	● 124.2	● 126.2	● 129.5	●
2	● 78.5	—	● 113.4	● 114.9	● 116.5	● 120.2	● 124.4	●
4	● 79.2	● 91	● 104	● 111.1	● 112.6	—	● 116.4	●
6	● 68.7	● 93.5	● 100.5	● 108.5	● 109.7	—	● 112	●
8	● 64.9	● 94.2	—	● 105.1	● 106.6	—	● 107.3	●
10	● 72.7	● 96.1	—	● 102.2	● 103.1	—	● 104.6	●

Table 1. (c) Transition temperatures (°C) of compounds of series C_n-FF-. The meanings of the signs used in this table are: C, crystalline phase; I isotropic phase; S_A, smectic A phase; S_C^{*}, helical smectic C phase; TGB_A, twist grain boundary smectic A phase; N*, cholesteric phase; BPI, blue phase I; BPIII, blue phase III; ●, the phase exists; —, the phase does not exist.

<i>n</i>	C	S _C [*]	S _A	TGB _A	N*	BPI	BPIII	I
7	● 91.5	—	● 107.4	● 108.8	● 141.3	● 142.4	● 144.6	●
8	● 92.2	—	● 115	● 115.9	● 140.2	● 141.3	● 143.5	●
9	● 78.7	—	● 113.9	● 115.1	● 134.2	● 135.8	● 138.2	●
0	● 81.8	—	● 116.7	● 117.7	● 132.9	● 134.3	● 136.7	●
1	● 78.6	—	● 114.6	● 116.2	● 128	● 129.4	● 132.5	●
2	● 72	—	● 113.3	● 115.9	● 125.4	● 127.3	● 130.2	●
4	● 90.9	● 106.3	—	● 109.9	● 117.6	● 120	● 123.4	●
6	● 77.6	● 101	—	● 111.7	● 113.7	● 115.7	● 119	●
8	● 79.4	● 99.3	—	● 110	● 111.1	● 112.5	● 115.3	●
10	● 81.3	● 94.9	—	● 99.5	● 103.1	● 104.8	● 108.7	●

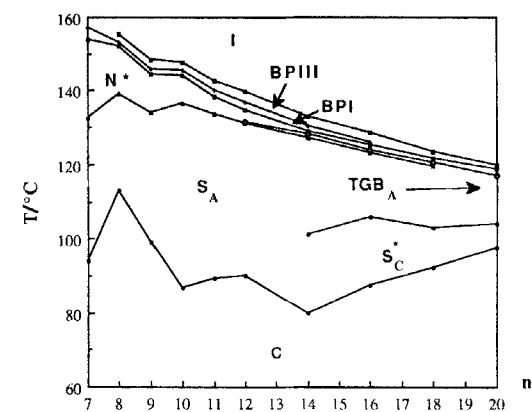
3.1. Optical microscopy

3.1.1. Series C_n-HH-

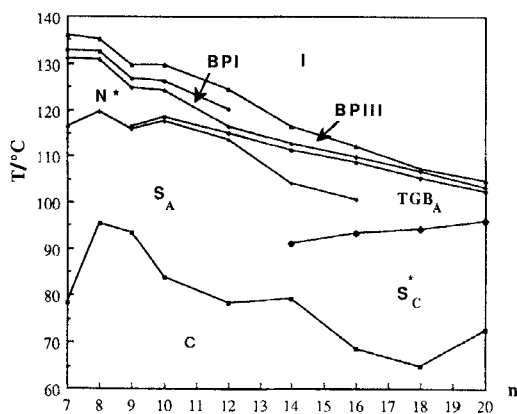
The first five derivatives ($n=7-11$) display blue phases, the cholesteric (N*) phase and the classical smectic A phase with focal-conic or homeotropic textures (see table 1(a) and figure 1(a)). Blue phase III (BPIII) is very difficult to observe under the microscope, but easily detected by calorimetric studies. The transition from BPIII to blue phase I (BPI) with a grazed platelet texture is very clear. The cholesteric phase appeared with the focal-conic or Grandjean plane texture. The TGB_A phase, below the cholesteric phase is obtained from $n=11$ to $n=20$ with a cholesteric texture, and dechiralization lines are observed at the TGB_A-S_A transition. The ferroelectric S_C^{*} phase, only observed with very long chains, appears from $n=14$ to 20. The S_C^{*} phase has two typical textures: striated fan or pseudo-homeotropic textures.

3.1.2. Series C_n-FH-

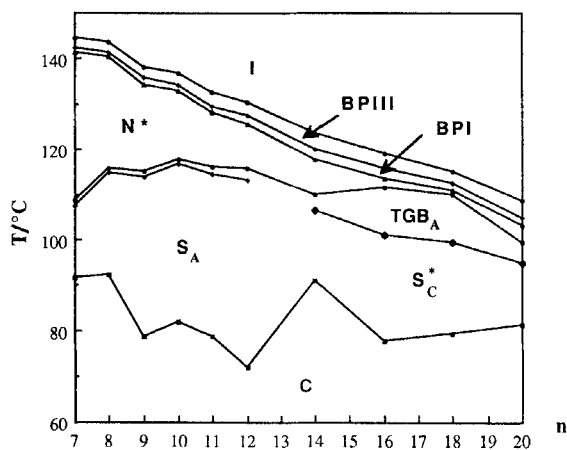
This series differs structurally from the A series, by the presence of the fluorine *meta*-to the COO group. On cooling from the isotropic liquid, all the compounds exhibit BPIII and a cholesteric phase. The TGB_A and S_C^{*} phases appear respectively for $n \geq 9$



(a)



(b)



(c)

Figure 1. Plots of transition temperatures versus n , the number of carbon atoms in the terminal chain: (a) $C_n\text{-HH-}$ series; (b) $C_n\text{FH-}$ series; (c) $C_n\text{-FF-}$ series.

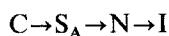
and $n \geq 14$. The classical S_A and BPI phases disappear respectively for $n \geq 18$ and $n \geq 14$. For all mesophases, the textures are the same as those for series C_n-HH-. The clarification and TGB_A-S_A transition temperatures are lower than those for the C_n-HH- series (see table 1 (b) and figure 1 (b)).

3.1.3. Series C_n-FF-

This series, with two fluorines substituted on the first benzene ring, shows the same mesomorphic properties as the C_n-HH- and C_n-FH- series. All homologues exhibit the cholesteric phase, two blue phases (BPI and BPIII) and the TGB_A phase. The classical S_A phase is obtained from $n = 7$ to $b = 12$. The ferroelectric S_C* phase is observed for $n \geq 14$. The transition temperatures are intermediate between those of hydrogenous and monofluorinated derivatives (see table 1 (c) and figure 1 (c)).

3.2. Racemic mixtures

The layered structure of the TGB_A phase is first inferred from studies of racemic mixtures of the three compounds: C12-HH-, C12-FH- and C12-FF-. They all exhibit the phase sequence:



(see table 2).

The TGB_A phase disappears in favour of a smectic A phase when chirality is eliminated in a racemic mixture. This shows that the TGB_A phase is a variant of the S_A phase. The temperatures of clarification are higher than those of the optically pure compounds. This result agrees well with the chiral NAC Renn-Lubensky model [3] and with the prediction of de Gennes [1].

3.3. Calorimetric studies

Transition enthalpies were determined by differential scanning calorimetry using a Perkin-Elmer DSC 7. The transition temperatures and corresponding enthalpies values are given in table 3. The temperatures are slightly different from those presented in tables 1 (a), (b) and (c), but the phase sequence is preserved. The thermograms were recorded upon heating at a rate of 1°C min⁻¹ (see figures 2 (a), (b), (c) and 3 (a), (b), (c)). Although slightly overlapping, the different phase transitions: S_A to TGB_A, TGB_A to N*, N* to BPI, BPI to BPIII and BPIII to I are clearly distinguished within a temperature range of 10°C.

It is very difficult to obtain separate transition enthalpies. Only the melting transition enthalpies are easy to determine unambiguously. They range from 40 to 60 kJ mol⁻¹. We give the sum for the S_A-TGB_A and TGB_A-N* transitions. The transition enthalpies are weak, between 0.04 and 0.5 kJ mol⁻¹ and decrease with the chain length. The last three temperatures (N* to BPI, BPI to BPIII and BPIII to I) slightly increase with chain length.

Table 2. Transition temperatures (°C) of pure compounds and racemic (Rac) mixtures.

Compounds	C	S _A	TGB _A	N* or N	I
C12-HH- (R) or (S)	● 90	● 131	● 131.6	● 139.7	●
Racemic	● 99.5	● 131.9	—	● 140.5	●
C12-FH- (R) or (S)	● 78.5	● 113.4	● 114.9	● 116.6	●
Racemic	● 66.4	● 115.5	—	● 117.4	●
C12-FF- (R) or (S)	● 72	● 113.3	● 114.5	● 130.2	●
Racemic	● 76.5	● 116.6	—	● 131.1	●

Table 3. Calorimetric studies with C14-HH-, C14-FH-, C14-FF-, and C18-HH-C18-FH-, C18-FF-,

Compounds	C	S _C	S _A	TGB _A	N*	BPI	BPIII	I
C14-HH-	•	77.8 (41.8)†	•	124.9 (0.5)‡	•	127.1 (2.1)	•	131.1 •
C14-FH-	•	78.5 (50.7)†	•	106.2 (0.4)‡	•	109.3 (1.7)	•	114.5 •
C14-FF-	•	90.5 (53.4)†	—	•	110.8 (0.6)§	•	118 •	121.2 •
C18-HH-	•	90.2 (61.3)†	•	117.9 (0.04)‡	•	119.8 (3.2)	•	121.4 •
C18-FH-	•	61.6 (35.2)†	—	•	103.8 (0.3)§	•	105.3 •	106.9 •
C18-FF-	•	76.1 (52.6)†	•	99.3	•	109.2 (1.8)	•	113.5 •
					•	110.7 (0.8)	•	

†ΔH(C-S_C); ‡ΔH(S_A-TGB_A-N*); §ΔH(TGB_A-N*); ||ΔH(N*-BPI-BPIII-I).

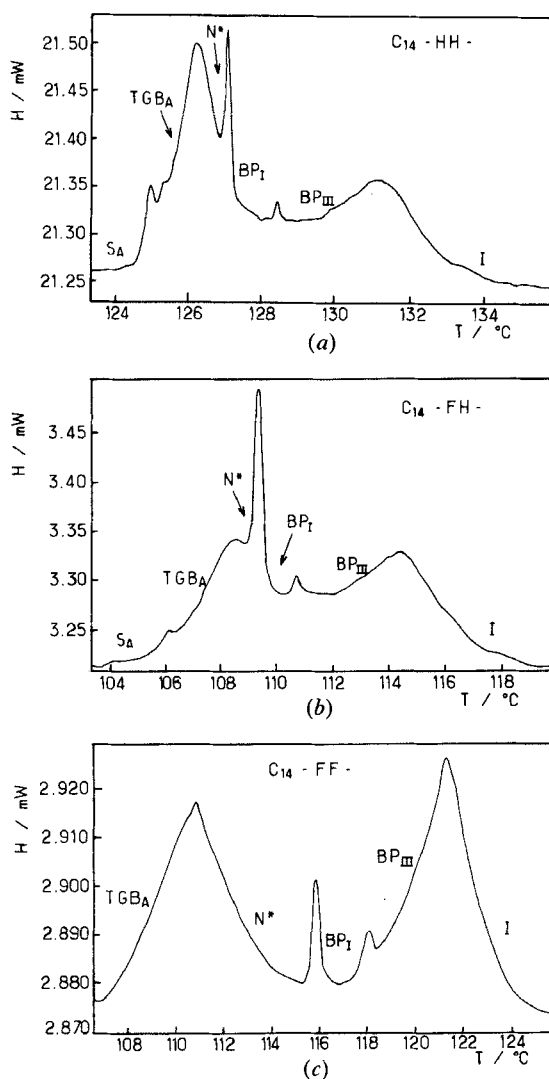


Figure 2. Differential scanning calorimetry thermograms for heating cycles with compounds (a) C₁₄-HH- compound (rate = 1°C min⁻¹); (b) C₁₄-FH- compound (rate = 1°C min⁻¹); (c) C₁₄-FF- compound (rate = 1°C min⁻¹).

4. X-ray scattering

X-ray scattering experiments were performed on powder (i.e. non-oriented) samples. Three compounds were studied: C18-HH-, C18-FH- and C18-FF-. The samples were prepared in 1 mm diameter Lindemann capillaries. The scattered intensities were collected with a 2θ goniometer, using CuK _{α} radiation from an 18 kW rotating anode X-ray generator. A flat pyrolytic graphite (002) monochromator delivered a $0.6 \times 2 \text{ mm}^2$ beam on to the sample. The scattered radiation was analysed by 0.6 mm vertical slits. The horizontal resolution was then $7 \times 10^{-3} \text{ \AA}^{-1}$ FWHM. The 2θ scans exhibited Bragg reflections with an asymmetrical profile due to a strong enhancement of the high q side of the peaks in the TGB_A and N* phases. In this latter case, the broad Bragg reflections correspond to short range smectic order. As already

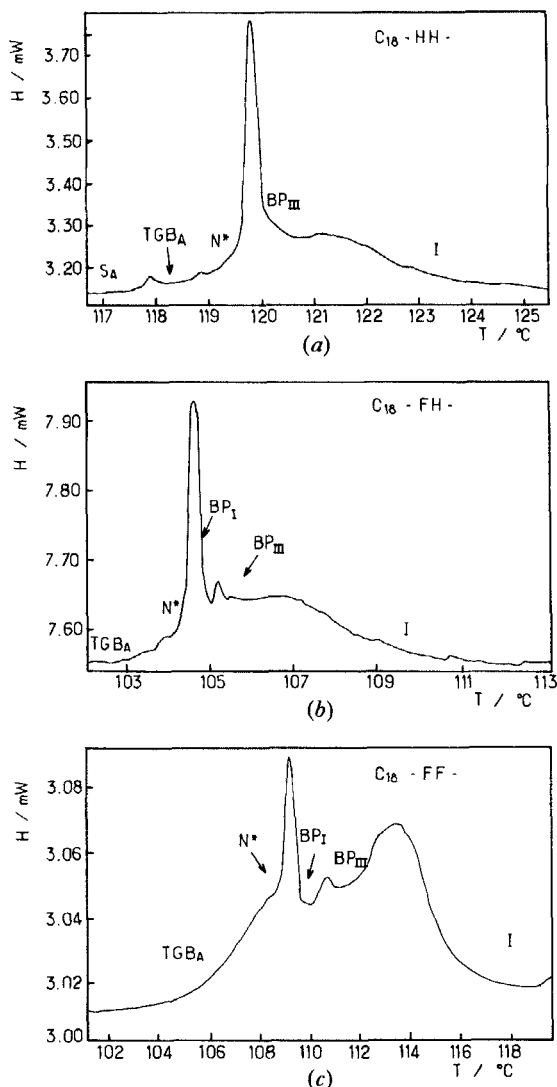


Figure 3. Differential scanning calorimetry thermograms for heating cycles. Rate = $1^{\circ}\text{C min}^{-1}$
 (a) C18-HH-; (b) C18-FH-; (c) C18-FF-.

explained [10], the peaks were fitted with the anisotropic structure factor given by Renn and Lubensky [2] after powder averaging and convolution with the (gaussian) resolution function. Although other effects (such as S_C like fluctuations) may contribute to the observed asymmetry of the peaks, it is almost impossible to distinguish its exact origin with a powder sample. Besides, the TGB structure factor (i.e. gaussian along the pitch axis) and the cholesteric structure factor (gaussian along the pitch, lorentzian along the other two directions [2] fit the data well in the TGB_A and N^* phases, respectively. Figures 4 (a), (b) and (c) give the variation of the layer spacing d ($d = 2\pi/q_0$) with temperature.

Upon heating the C18-HH- homologue from the S_C^* phase, the layer spacing exhibits a continuous increase from 44.4 \AA at 97°C to 45.3 \AA in the S_A phase at 103°C .

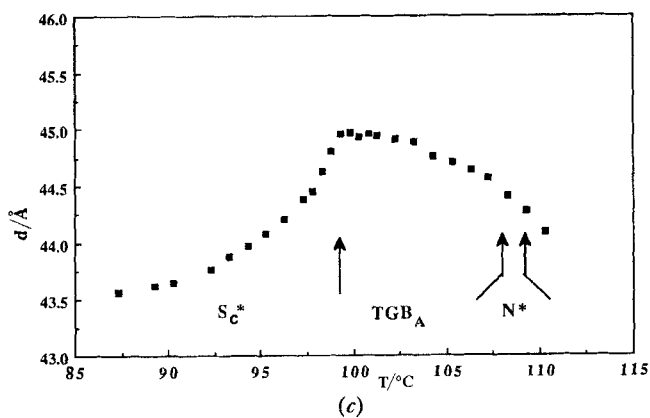
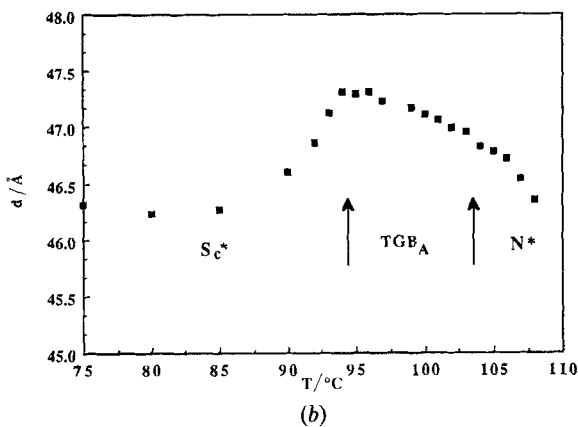
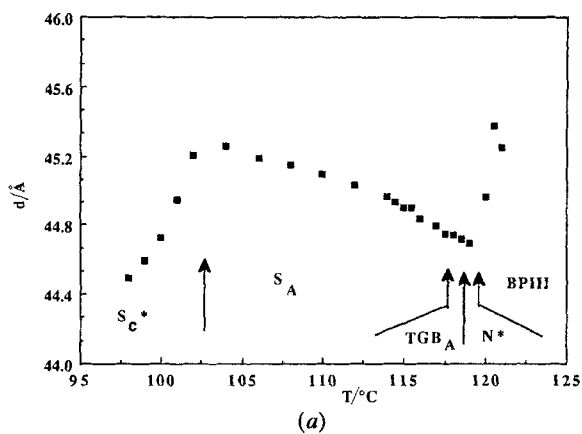


Figure 4. Layer spacing versus temperature as obtained from X-ray scans for three homologues: (a) C18-HH-; (b) C18-FH-; (c) C18-FF-.

Then, the layer spacing decreases from 45.3 Å in the TGB_A phase to 44.6 Å in the cholesteric phase at 119.8°C. The S_A - TGB_A and the TGB_A - N^* transitions are not visible on the plots of figure 4 (a). Note that the short smectic spacing is still visible in the blue phase (BPIII) and that the layer spacing increases sharply above the N^* -BPIII transition.

The C18-FH- homologue exhibits the phase sequence: S_C^* - TGB_A - N^* upon heating. Figure 4 (b) show the evolution of the layer spacing as a function of temperature. Like the C18-HH- homologue, the layer spacing increases from 46.3 Å to 47.4 Å in the N^* . Note that the width of the Bragg peak becomes larger in the TGB_A phase.

Figure 4 (c) shows that the layer spacing of the C18-FF- homologue exhibits a continuous increase upon heating from 43.5 Å in the S_C^* phase up to 45 Å in the TGB_A phase. It then decreases regularly, without any anomaly, from the TGB_A (45 Å) to the cholesteric phase (44.5 Å).

At this stage, we observe that the results turn out to be very similar to those reported for a previous series [10] without any discontinuity. Two features are observed for all compounds:

- (1) The layer spacing remains always significantly shorter than the length of a molecule (l) in its most extended configuration. (C18-HH-, C18-FH- and C18-FF-, $l = 52.5$ Å.)
- (2) The layer spacing decreases gently from TGB_A to N^* phase upon heating.

These two observations can be simply explained by a folding of the flexible alkyl chains to fill space in between the rigid cores [6] (remember that the chiral chain is shorter than the alkyloxy chain). This effect increases with thermal motion of the cores.

The sharp increase observed for the C18-HH- homologue at 120°C in BPIII is unexplained.

5. Helical pitch measurements

Helical pitch measurements were performed using a Grandjean-Cano wedge for the cholesteric and TGB_A mesophases, whereas homeotropic drops were used for the smectic C^* phase.

The Grandjean-Cano wedge is made of two thoroughly cleaned and gently buffed glass plates which promote a planar alignment of the director at the surfaces along the buffing direction (perpendicular to the arête of the prism). The cell is filled with the material in its cholesteric phase by capillarity. The angle of the wedge is inferred from observation of the fringes of equal thickness given by the empty cell. It is always less than 1°.

Figures 5 (a), (b) and (c) show the evolution of the pitch as a function of temperature for the cholesteric and TGB_A mesophases of the C18-HH-, C18-FH- and C18-FF- compounds. All three materials exhibit the same kind of behaviour in the cholesteric, TGB_A and S_C^* phases.

For the hydrogenous compound (see figure 5 (a)), the pitch increases continuously from 0.3 to 0.95 μm upon cooling through the cholesteric phase, then rises steeply in the TGB_A phase up to 2.7 μm at the TGB_A - S_A transition. The pitch was measured on heating the S_C^* phase below 119.9°C using homeotropic drops. It varies continuously from 0.8 μm at 95°C up to 0.95 μm at 101°C then falls sharply down to 0.4 μm 1°C below the S_C^* - S_A transition.

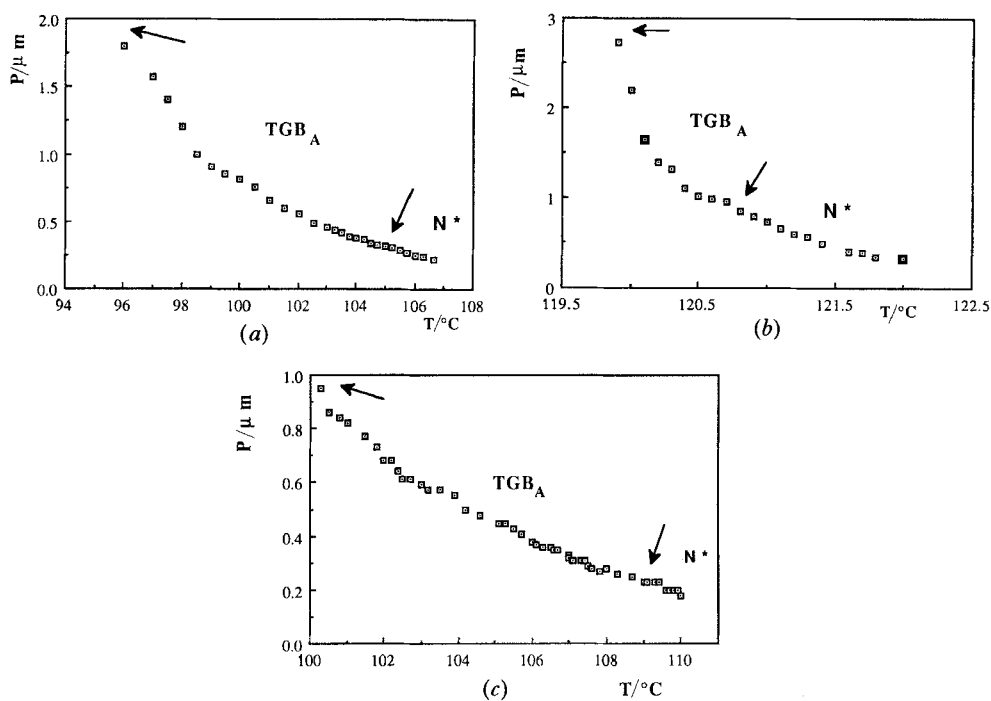


Figure 5. Helical pitch of the TGB_A and N* phases versus temperature for the series (a) Cn-HH-; (b) Cn-FH-; (c) Cn-FF-.

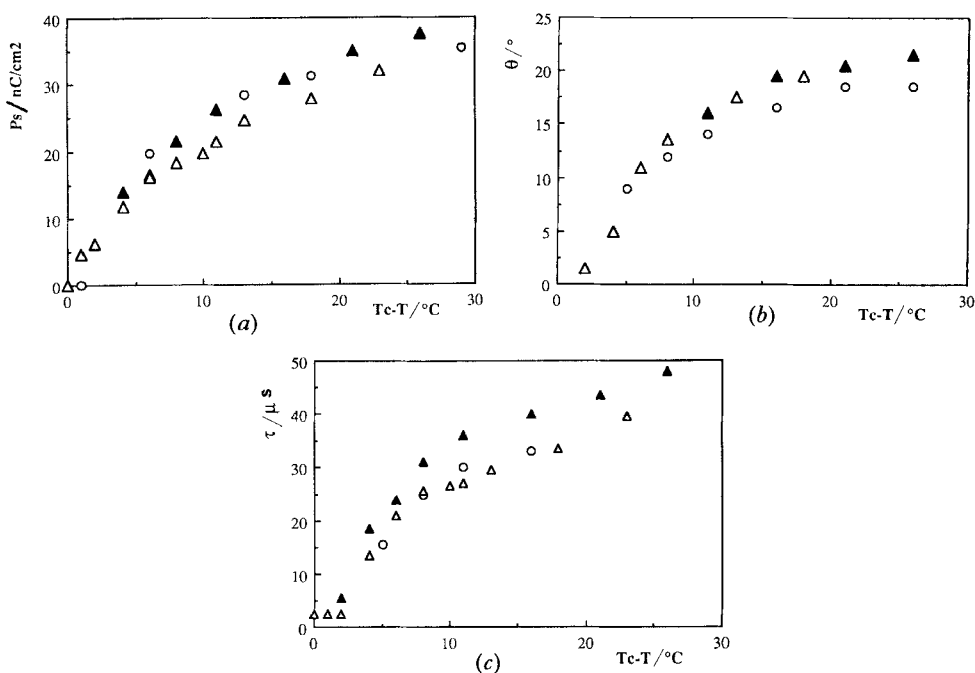


Figure 6. Influence of the aliphatic chain length: C14-HH- (○), C16-HH- (▲) and C18-HH- (△). (a) Polarization versus temperature. (b) Tilt angle versus temperature. (c) Response time versus temperature.

For the C18-FH- compound, the observed values are significantly lower (see figure 5(b)). They range from 0.28 to 0.53 μm on cooling the cholesteric phase. No discontinuity is detected at the N^*-TGB_A transition and the pitch increases quickly up to 1.8 μm at the $\text{TGB}_A-\text{S}_C^*$ transition. Accurate measurements turn out to be difficult for the TGB_A phase because of its high viscosity.

The behaviour in the S_C^* phase is quite similar to the hydrogenous compound: the pitch increases regularly on heating from 0.65 at 80°C to 0.75 μm at 93°C and drops abruptly down to 0.35 μm 1°C below the $\text{S}_C^*-\text{TGB}_A$ transition.

Lastly, C18-FF appears to be very similar to C18-FH, as shown in figure 5(c).

6. Electro-optical properties

We have studied the electro-optical properties of the S_C^* phase of these new compounds in the surface stabilized ferroelectric liquid crystal configuration (SSFLC) [12], including the temperature dependence of the response time, polarization and tilt angle. The applied voltage corresponding to saturation [13] is 30 V and recurrence frequency is 2 kHz. (For tilt angle measurements, $V = 25$ V and $\nu = 0.2$ Hz.)

Figures 6(a), (b) and (c) show the influence of the aliphatic chain length in the $\text{C}_n\text{-HH-}$ series; polarization, tilt angle and response time do not depend too much on chain length. These results show quite a high polarization (about 50 nC cm^{-2}), a slow response time (30 μs) and a saturated tilt angle of 20°.

Polarization, tilt angle and response time measurements are reported in figure 7(a), (b) and (c) for the C18-HH-, C18-FH- and C18-FF- compounds. We observe

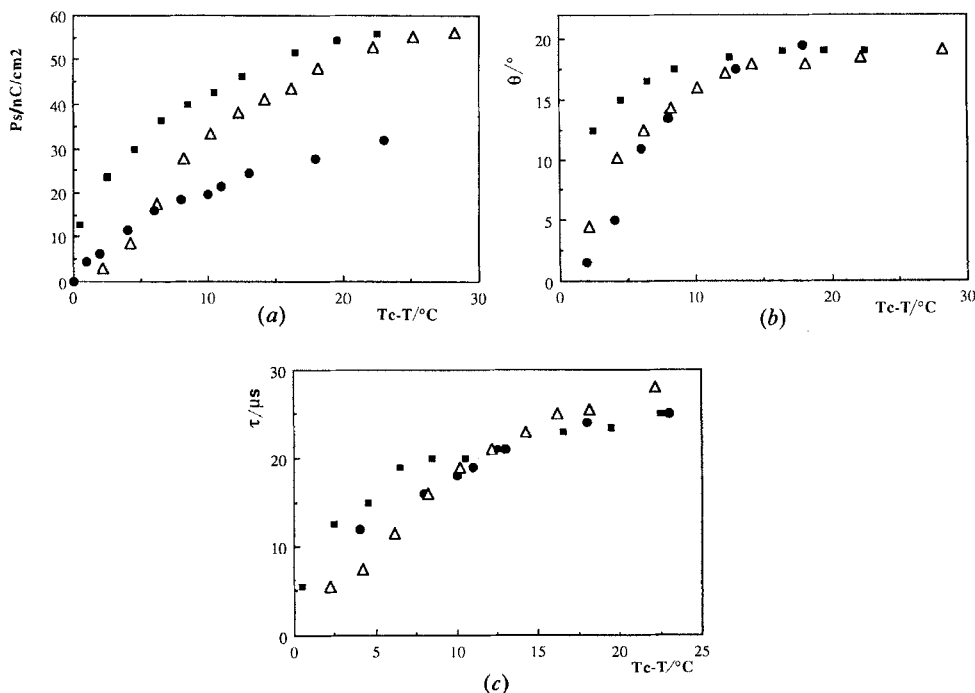


Figure 7. Influence of the number of fluorine substituents: C18-HH- (●), C18-FH- (Δ) and C18-FF- (■). (a) Spontaneous polarization versus temperature. (b) Tilt angle versus temperature. (c) Response time versus temperature.

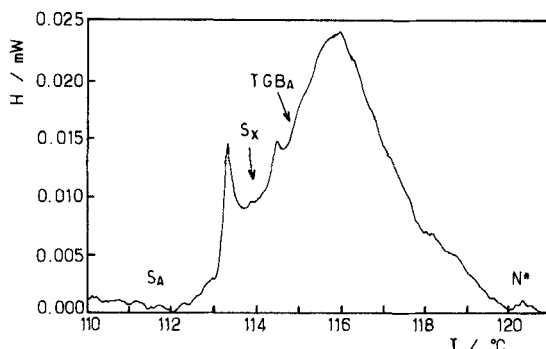


Figure 8. Differential scanning calorimetry thermogram for a heating cycle on compound C12-FF-.

that the spontaneous polarization increases with the number of fluorine atoms. The influence of fluorine on tilt angle and response time values is, however, insignificant.

All these values are comparable with those reported for other compounds exhibiting the TGB_A phase [6, 9, 10].

7. Conclusion

All compounds in the three new series are mesomorphic. The predicted phase sequence, that is to say S_A-TGB_A-N* is found in the three series for several compounds. The presence of two fluorines substituted on the first benzene ring favours TGB_A phase formation. Temperatures of transition are lower for the C_n-FH- series than for the C_n-HH- and C_n-FF- series. It is very difficult to obtain enthalpy values for many of the transitions. Note that the C_n-FF- series presents an anomaly for $n = 7$ to 12 homologues. We can see (figure 8) that the thermogram for the C12-FF- compound shows a new thermal event between the S_A-TGB_A and TGB_A-N* transition ($T = 114.5^\circ\text{C}$). We tried to characterize a possible new phase by different methods: microscopic observations and racemic mixture studies, but we have not observed any other evidence of a new transition. Further experimental studies of this compound are currently in progress.

Layer spacing values obtained from X-ray diffraction studies on the C18-HH-, C18-FH- and C18-FF- homologues are shorter than the molecular length, as already observed for other series [10]. The pitch is shorter than for other series [6, 9, 10]. In terms of superconductor analogy, this corresponds to a higher magnetic field and may therefore generate high densities of vortices (i.e. screw dislocations) in the Abrikosov (i.e. TGB) phase. As expected from the Renn-Lubensky model, the pitch increases strongly in the TGB phase upon approaching the smectic A phase. The spontaneous polarization of the S_C^{*} phase of these new compounds increases with aliphatic chain length and with the number of fluorine atoms. The values are quite high, about 50 nC cm^{-2} . The tilt angle and response time are insensitive to these two parameters.

8. Experimental section

Infrared spectra were recorded using a Perkin-Elmer 783 spectrophotometer and NMR spectra with a Bruker 270 MHz spectrometer. All the compounds gave satisfactory analyses.

8.1. *(R)*-(1-Ethoxycarbonyl)ethyl 4-iodobenzoate

To a cooled solution of 4-iodobenzoic acid (17.4 g; 50 mmol), (*S*)-ethyl lactate (7.1 g; 60 mmol), and triphenylphosphine (TTP) (14.42 g; 55 mmol) in CH_2Cl_2 (100 ml) was added dropwise diethyl azodicarboxylate (DEAD) (9.6 g; 55 mmol) [14]. The solution was stirred at room temperature for 2 h. The solution was filtered, evaporated and chromatographed on silica gel with toluene as eluent. The desired compound was crystallized from heptane. Yield 13.8 g (66 per cent), m.p. = 33.9°C. $^1\text{H NMR}$ (CDCl_3 , δ): 1.3 (t, 3 H, $\text{CH}_3\text{-CH}_2\text{-O}_2\text{C}$), 1.6 (d, 3 H, $\text{CH}_3\text{-CH}$), 4.2 (q, 2 H, $\text{CH}_3\text{-CH}_2\text{-O}_2\text{C}$), 5.3 (q, 1 H, CH-CH_3), 7–8 (m, 4 H arom). IR (Nujol): 1745, 1730, 1580, 830 cm^{-1} .

8.2. *(S)*-(1-Ethoxycarbonyl)ethyl 4-iodobenzoate

To a solution of (*S*)-ethyl lactate (5.9 g; 50 mmol), dicyclohexylcarbodiimide (DCC) (11.35 g; 55 mmol) and 4*N,N*-dimethylaminopyridine (DMAP) (1 g) in CH_2Cl_2 (300 ml) was added 4-iodobenzoic acid (12.4 g; 50 mmol). The mixture was stirred at room temperature overnight. The solution was filtered, evaporated and chromatographed on silica gel with toluene as eluent. Yield 10.4 g (60 per cent).

8.3. *(R)*-4-Carboxyloxy-(1-ethoxycarbonyl)ethyl-4'-hydroxytolane

In a 250 ml round bottomed flask were placed 4-(tetrahydropyranyloxy)-phenylacetylene [9] (5.8 g; 28 mmol), (*R*)-(1-ethoxycarbonyl)ethyl 4-iodobenzoate (10 g; 28 mmol) and TPP (0.26 g; 1 mmol) in diisopropylamine (40 ml). The solution was stirred and heated in a oil bath at 30°C until complete dissolution. Then the catalysts PdCl_2 (30 mg) and $\text{Cu}(\text{AcO})_2 \cdot \text{H}_2\text{O}$ (32.5 mg) were added to this solution which was gradually heated to 90°C and maintained at this temperature for 4 h [15]. After cooling to room temperature, the salt was removed by filtration and washed well with ethyl acetate. The filtrate was evaporated and hydrolysed with concentrated hydrochloric acid (8 ml), water (100 ml) and crushed ice (50 g) and then shaken with ethyl acetate. The organic phase was dried over anhydrous Na_2SO_4 , was filtered and evaporated. The residue was chromatographed on silica gel, eluting with (8:2) heptane-ethyl acetate mixture. The protected intermediate was dissolved in a CH_2Cl_2 (70 ml): CH_3OH (100 ml) mixture. To this solution was added 4-toluenesulphonic acid (PTSA) (0.2 g) and the mixture was stirred at room temperature for 1 h. The solvent was removed and the pure phenol obtained by chromatography on silica gel with (8:2) heptane-ethyl acetate mixture. Yield 7 g (76 per cent), m.p. = 119.8°C. $^1\text{H NMR}$ (CDCl_3 , δ): 1.3 (t, 3 H, $\text{CH}_3\text{-CH}_2\text{-O}_2\text{C}$), 1.6 (d, 3 H, $\text{CH}_3\text{-CH}$), 4.2 (q, 2 H, $\text{CH}_3\text{-CH}_2\text{-O}_2\text{C}$), 5.3 (q, 1 H, CH-CH_3), 6.4 (s, 1 H of OH), 6.8–8 (m, 8 H arom). IR (Nujol): 3400, 2200, 1710, 1600, 830 cm^{-1} .

8.4. *(R)*-4-(Carboxyloxy-(1-ethoxycarbonyl)ethyl)-4'-(4-dodecyloxybenzoyloxy)tolane

To a solution of the precursor phenol (680 mg; 2 mmol) in CH_2Cl_2 (5 ml) was added DCC (450 mg; 2.2 mmol), DMAP (40 mg) and 4-dodecyloxybenzoic acid (673 mg; 2.2 mmol). The mixture was stirred at room temperature overnight. It was then filtered, evaporated and the product chromatographed on silica gel with CH_2Cl_2 as eluent. The required compound was crystallized from absolute ethanol. Yield 1.6 g (68 per cent). Transition temperatures: $\text{C}90^\circ\text{C S}_A$ 131°C TGB_A 131.6°C N^* 134.9°C BPI $136.9^\circ\text{C BPIII}$ 139.7°C I . $^1\text{H NMR}$ (CDCl_3 , δ): 0.8 (t, 3 H, $\text{CH}_3\text{-(CH}_2\text{)}_{11}\text{-}$), 1.3 (m, 19 H, $\text{-(CH}_2\text{)}_8\text{-CH}_2\text{-CH}_3$), 1.4 (m, 2 H, $\text{(CH}_2\text{)}_\gamma\text{-}$), 1.6 (d, 3 H, $\text{CH}_3\text{-CH}$), 1.8 (q, 2 H, $\text{(CH}_2\text{)}_\beta$), 4 (t, 2 H, $\text{CH}_2\text{-O}$), 4.2 (q, 2 H, $\text{CH}_2\text{-CH}_3$), 5.3 (q, 1 H, CH-CH_3), 7.9–8.1 (6d, 12 H arom). IR (Nujol): 1750, 1740, 1720, 1610, 830 cm^{-1} .

References

- [1] DE GENNES, P. G., 1972, *Solid St. Commun.*, **10**, 753.
- [2] RENN, S. R., and LUBENSKY, T. C., 1988, *Phys. Rev. A*, **38**, 2132.
- [3] RENN, S. R., and LUBENSKY, T. C., 1991, *Molec. Crystals liq. Crystals*, **209**, 349.
- [4] RENN, S. R., 1992, *Phys. Rev. A*, **45**, 953.
- [5] GOODBY, J. W., WAUGH, M. A., STEIN, S. M., CHIN, E., PINDAK, R., and PATEL, J. S., 1989, *J. Am. chem. Soc.*, **111**, 8119.
- [6] NGUYEN, H. T., TWIEG, R. J., NABOR, M. F., ISAERT, N., and DESTRADE, C., 1991, *Ferroelectrics*, **121**, 187.
- [7] LAVRENTOVICH, O. D., NASTISHIN, Y. A., KULISHOV, V. I., NARKEVICH, Y. S., TOLOCKA, A. S., and SHIYANOVSKII, S. V., 1990, *Europhysics Lett.*, **13**, 313.
- [8] SLANEY, A. J., and GOODBY, J. W., 1991, *J. mater. Chem.*, **1**, 5.
- [9] BOUCHTA, A., NGUYEN, H. T., ACHARD, M. F., HARDOUIN, F., DESTRADE, C., TWIEG, R. J., MAAROUI, A., and ISAERT, N., 1992, *Liq. Crystals*, **12**, 575.
- [10] NGUYEN, H. T., BOUCHTA, A., NAVAILLES, L., BAROIS, P., ISAERT, N., TWIEG, R. J., MAAROUI, A., and DESTRADE, C., 1992, *J. Phys., Paris*, **2**, 1889.
- [11] KELLY, S. M., 1989, *Helv. chim. Acta*, **72**, 594.
- [12] NABOR, M. F., NGUYEN, H. T., DESTRADE, C., MARCEROU, J. P., and TWIEG, R. J., 1991, *Liq. Crystals*, **10**, 785.
- [13] CLARK, N. A., and LAGERWALL, S. T., 1980, *Appl. Phys. Lett.*, **36**, 899.
- [14] MITSUNOBU, O., and EGUCHI, M., 1971, *Bull. chem. Soc. Japan*, **44**, 3427.
- [15] AUSTIN, W. B., BILOW, N., KELLEGHAN, W. J., and LAU, K. S. Y., 1981, *J. org. Chem.*, **46**, 2280.